ELSEVIER

Inorganica Chimica Acta 226 (1994) 267–274

Inorganica Chimica Acta

# Synthesis, molecular structure and electrochemical investigation of the 1,2,5-thiadiazole-3,4-dithiolate-substituted complex Cp*Ru(NO)(tdas). Evidence for nitrosyl bending during reduction

Chun-Gu Xia [a], Simon G. Bott [b,*], Michael G. Richmond [b,*]

[a] *Lanzhou Institute of Chemical Physics, Academia Sinica, Lanzhou 730000, People's Republic of China*

[b] *Center for Organometallic Research and Education, Department of Chemistry, University of North Texas, Denton, TX 76203, USA*

Received 23 March 1994

**Abstract**

Treatment of disodium 1,2,5-thiadiazole-3,4-dithiol ($Na_2$tdas) with the cyclopentadienyl complex Cp*Ru(NO)$Cl_2$ in MeOH gives the corresponding 1,2,5-thiadiazole-3,4-dithiolate-substituted complex Cp*Ru(NO)(tdas) in 61% yield. The product has been characterized in solution by IR and NMR ($^1$H and $^{13}$C) spectroscopies, and the molecular structure of Cp*Ru(NO)(tdas) has been established by X-ray diffraction analysis. Cp*Ru(NO)(tdas) crystallizes in the monoclinic space group $P2_1/c$ with $a=26.204(2)$, $b=8.4915(6)$, $c=14.2339(9)$ Å, $\beta=90.739(5)°$, $V=3166.9(3)$ Å$^3$ and $Z=8$. Full-matrix least-squares refinement yielded $R=0.0338$ for 3151 ($I>3\sigma(I)$) reflections. The redox properties of Cp*Ru(NO)(tdas) were examined by cyclic and rotating disk electrode voltammetric techniques. Two electrochemical responses were observed and assigned to $0/+1$ and $0/-1$ redox couples. Both of these redox couples are quasi-reversible. It is suggested that the stability of the $0/-1$ redox couple is modulated by an EC scheme, whereby the initial reduction product $[Cp^*Ru(NO)(tdas)]^{\cdot-}$ undergoes a bending of the nitrosyl ligand. The nitrosyl bending is observable at low temperature in THF solvent. The nature of the HOMO and LUMO levels in Cp*Ru(NO)(tdas) has been determined by extended Hückel molecular orbital calculations, the results of which are discussed with respect to the electrochemical data.

*Keywords:* X-ray diffraction analysis; Voltammetric techniques; Hückel molecular orbital; Nitrosyl bending; Cyclopentadienylruthenium complexes

## 1. Introduction

The chemistry of organometallic complexes bearing chelating dithiolate ligands has been thoroughly reviewed over the last few years [1–3]. Interest in this genre of compounds stems from the existence of unusual solid-state properties [4], analytical chemistry applications [5] and luminescence behavior in fluid solution that have been reported [6]. Of the many dithiolate complexes that have been synthesized and structurally characterized, few complexes based on the 1,2,5-thiadiazole-3,4-thiolate (tdas) ligand are known. Only recently have metal complexes with a tdas ligand been synthesized and explored for their redox and solid-state conducting properties. The synthesis of $[M(tdas)_2]^{n-}$ (where M = Ni, Pd, Pt, Cu; $n=2$) and $[Fe(tdas)_2]^-$ by Hawkins and Underhill has provided promising evidence for the construction of semiconducting materials when these tdas complexes are electrooxidized with tetrathiafulvalene [7]. More recently, Cassoux and co-workers have published the first X-ray crystallographic structures of the tdas-substituted nickel complexes $[Ni(tdas)_2][R_4N]_2$ (where R = Et, Bu). In this particular study, the differences between the crystal structures were discussed with respect to the gegencation [8].

Here we report our results on the first tdas-substituted cyclopentadienylruthenium complex Cp*Ru(NO)(tdas). Included in our report are the X-ray crystal structure and the electrochemical properties of Cp*Ru(NO)(tdas). The results of extended Hückel molecular orbital calculations on Cp*Ru(NO)(tdas) are also presented and discussed in relationship to the observed redox data.

* Corresponding authors.

0020-1693/94/$07.00 © 1994 Elsevier Science S.A. All rights reserved
*SSDI* 0020-1693(94)04095-D

## 2. Results and discussion

### 2.1. Synthesis and solution characterization of Cp*Ru(NO)(tdas)

The reaction between equimolar amounts of $Cp^*Ru(NO)Cl_2$ [9] and disodium 1,2,5-thiadiazole-3,4-dithiolate ($Na_2tdas$) [10,11] proceeds slowly in MeOH solution at room temperature, as outlined in Eq. (1). After stirring the reaction solution overnight, the desired tdas-substituted product, Cp*Ru(NO)(tdas), could be isolated in 61% yield by chromatography over silica gel using $CH_2Cl_2$ as the eluant. While complex **2** is insoluble in common saturated hydrocarbon solvents, it is soluble in toluene, MeCN and $CH_2Cl_2$. Complex **2** is stable in the solid state under argon for several weeks, but solutions of **2** decompose over a period of days when exposed to the atmosphere.

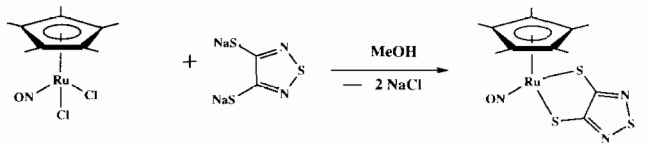


**2** (1)

The IR spectrum of **2** in $CH_2Cl_2$ exhibits a $\nu$(NO) band at 1769 $cm^{-1}$ in full agreement with the frequency reported for other organometallic complexes possessing a terminal nitrosyl ligand [12]. The $^1H$ NMR spectrum of **2** in $CDCl_3$ displays a single resonance at $\delta = 1.86$ for the methyl groups of the Cp* ligand while the $^{13}C$ NMR spectrum of **2** displays three resonances at $\delta = 9.5$, 109.5 and 169.6, which are assigned to the methyl, Cp* ring and the thiadiazole ring carbons, respectively.

### 2.2. X-ray crystallographic structure of Cp*Ru(NO)(tdas)

The molecular structure of Cp*Ru(NO)(tdas) was determined by X-ray diffraction analysis. Single crystals of **2** suitable for X-ray diffraction analysis were grown from a $CH_2Cl_2$ solution of **2** that had been layered with pentane. Cp*Ru(NO)(tdas) exists as discrete molecules in the unit cell with no unusually short inter- or intramolecular contacts. The X-ray data collection and processing parameters for **2** are listed in Table 1 with the fractional coordinates given in Table 2.

The packing diagram (not shown) reveals a pattern of alternating Cp* and thiadiazole rings between molecules of **2**, a situation that is reminiscent of the stacking pattern observed in many dithiolate donor–acceptor complexes [4,13]. The ORTEP diagram in Fig. 1 shows the molecular structure of one of the two molecules of **2** found in the unit cell while Table 3 lists selected bond distances and angles for **2**. The ruthenium atom in **2** has a six-coordinate geometry, assuming that the Cp* ring functions as a three-coordinate ligand. **2** possesses idealized $C_s$ molecular symmetry as observed with all three-legged piano-stool complexes that have two equivalent legs.

Table 1
X-ray crystallographic and data processing parameters for Cp*Ru(NO)(tdas) (**2**)

| | |
|---|---|
| Space group | monoclinic, $P2_1/c$ |
| Cell constants | |
| $a$ (Å) | 26.204(2) |
| $b$ (Å) | 8.4915(6) |
| $c$ (Å) | 14.2339(9) |
| $\beta$ (°) | 90.739(5) |
| $V$ (Å$^3$) | 3166.9(3) |
| Molecular formula | $C_{12}H_{15}N_3ORuS_3$ |
| Formula weight | 414.53 |
| Formula units/cell, $Z$ | 8 |
| $\rho$ (g $cm^{-3}$) | 1.739 |
| Crystal size ($mm^3$) | $0.05 \times 0.21 \times 0.32$ |
| Absorption coefficient, $\mu$ ($cm^{-1}$) | 13.49 |
| $\lambda$(radiation) (Å) | 0.71073 |
| Collection range (°) | $2.0 \leqslant 2\theta \leqslant 44.0$ |
| Total no. data collected | 4265 |
| No. independent observed data | 3151 |
| $R$ | 0.0338 |
| $R_w$ | 0.0373 |
| Weights, $w$ | $[0.04F^2 + (\sigma F)^2]^{-1}$ |

The Ru–S(thiolate) bond distances in both molecules of **2** range from 2.363(2) to 2.374(2) Å with a mean distance of 2.369 Å. These distances are in close agreement with those reported for the structurally related ruthenium dithiolate complex Cp*Ru(NO)(mnt) [14] and other metal dithiolate complexes [15]. An observed Ru–N(nitrosyl) distance of 1.755 Å (av.) is consistent with a terminal Ru–N(nitrosyl) bond [16]. Little perturbation on the nitrosyl ligand by the Cp* and the tdas rings is seen as the angle adopted by the Ru–N–O linkage of 170.1° (av.) deviates only slightly from the ideal angle of 180°. The tdas ring distances and angles in **2** compare favorably to those reported by Cassoux and co-workers for $[Ni(tdas)_2]^{2-}$ [8]. The remaining distances and angles in **2** are unexceptional and require no further comment.

### 2.3. Redox investigation of Cp*Ru(NO)(tdas)

All electrochemical studies on Cp*Ru(NO)(tdas) were carried out at a platinum electrode in either MeCN or THF solvent containing 0.25 M tetra-n-butylammonium perchlorate (TBAP) as the supporting electrolyte. The redox responses of Cp*Ru(NO)(tdas) in MeCN were examined by cyclic voltammetry (CV) and rotating disk electrode (RDE) voltammetry. In the cyclic voltammograms of **2** in MeCN two well-defined redox couples at $E_{1/2} = 0.99$ and $\sim -1.06$ V are observed at a scan rate of 100 mV $s^{-1}$ as a function of temperature,

Table 2
Positional parameters of the non-hydrogen atoms for Cp*Ru(NO)(tdas) (**2**) with e.s.d.s in parentheses

| Atom | x | y | z | $U^a$ |
|---|---|---|---|---|
| Molecule A | | | | |
| Ru1 | 0.10039(1) | 0.26332(7) | 0.24941(4) | 2.78(1) |
| S11 | 0.16574(5) | 0.2358(2) | 0.1369(1) | 3.60(4) |
| S12 | 0.07812(6) | −0.0016(3) | 0.2188(1) | 4.32(4) |
| S13 | 0.17791(8) | −0.2161(3) | 0.0413(2) | 6.04(5) |
| O1 | 0.0230(2) | 0.4406(8) | 0.1476(4) | 6.7(1) |
| N1 | 0.0539(2) | 0.3606(8) | 0.1808(4) | 4.0(1) |
| N12 | 0.1952(2) | −0.0297(9) | 0.0491(5) | 4.8(1) |
| N14 | 0.1273(2) | −0.2094(9) | 0.1101(5) | 5.2(2) |
| C11 | 0.1626(2) | 0.0396(9) | 0.1065(5) | 3.3(1) |
| C15 | 0.1244(2) | −0.0657(9) | 0.1407(5) | 3.7(1) |
| C101 | 0.0770(2) | 0.3136(8) | 0.3981(4) | 2.7(1) * |
| C102 | 0.1137(2) | 0.1923(8) | 0.4044(5) | 2.9(1) * |
| C103 | 0.1599(2) | 0.2547(9) | 0.3664(5) | 3.5(1) * |
| C104 | 0.1513(2) | 0.4115(9) | 0.3379(5) | 3.5(1) * |
| C105 | 0.0990(2) | 0.4509(9) | 0.3596(5) | 3.5(1) * |
| C111 | 0.0238(2) | 0.305(1) | 0.4397(6) | 4.5(2) |
| C112 | 0.1064(3) | 0.035(1) | 0.4464(6) | 4.5(2) |
| C113 | 0.2097(2) | 0.168(1) | 0.3656(6) | 5.8(2) |
| C114 | 0.1899(3) | 0.526(1) | 0.3004(2) | 5.5(2) |
| C115 | 0.0748(3) | 0.608(1) | 0.3491(7) | 5.3(2) |
| Molecule B | | | | |
| Ru2 | 0.63494(2) | 0.14240(7) | 0.95979(4) | 3.23(1) |
| S21 | 0.56718(6) | 0.2638(3) | 1.0406(1) | 4.75(4) |
| S22 | 0.68282(5) | 0.3769(2) | 0.9830(1) | 4.23(4) |
| S23 | 0.60594(7) | 0.6998(3) | 1.1404(2) | 5.29(5) |
| O2 | 0.6907(2) | −0.0323(8) | 1.1026(5) | 6.7(2) |
| N2 | 0.6658(2) | 0.0408(8) | 1.0512(4) | 4.3(1) |
| N22 | 0.5680(2) | 0.5487(9) | 1.1255(4) | 4.6(1) |
| N24 | 0.6552(2) | 0.6312(8) | 1.0827(5) | 4.6(1) |
| C21 | 0.5921(2) | 0.4433(9) | 1.0751(5) | 3.8(2) |
| C25 | 0.6425(2) | 0.4929(9) | 1.0509(5) | 3.5(1) |
| C201 | 0.5755(2) | 0.0978(9) | 0.8413(5) | 3.7(1) * |
| C202 | 0.6130(2) | 0.210(1) | 0.8199(6) | 4.5(1) * |
| C203 | 0.6616(2) | 0.125(1) | 0.8144(5) | 4.2(1) * |
| C204 | 0.6534(2) | −0.0284(9) | 0.8448(5) | 3.2(1) * |
| C205 | 0.6000(2) | −0.0436(8) | 0.8645(5) | 3.1(1) * |
| C211 | 0.5197(2) | 0.127(1) | 0.8413(6) | 6.0(2) |
| C212 | 0.6031(3) | 0.374(1) | 0.7812(7) | 6.6(2) |
| C213 | 0.7109(3) | 0.190(1) | 0.7736(6) | 5.6(2) |
| C214 | 0.6919(2) | −0.159(1) | 0.8532(6) | 4.9(2) |
| C215 | 0.5738(2) | −0.194(1) | 0.8929(6) | 4.8(2) |

* Anisotropically refined atoms are given in the form of the isotropic equivalent displacement parameter defined as: $(4/3)[a^2B_{1,1}+b^2B_{2,2}+c^2B_{3,3}+ab(\cos\gamma)B_{1,2}+ac(\cos\beta)B_{1,3}+bc(\cos\alpha)B_{2,3}$. Starred atoms were refined isotropically.

assignable to a one-electron oxidation and reduction, respectively. These cyclic voltammograms are shown in Fig. 2(a). All cyclic voltammograms were reproducible and only slight electrode passivation was noticed over prolonged investigation periods. Whereas the reduction wave does not display a major dependence on the temperature at which the CV is recorded, the oxidation couple becomes more stable as the temperature is lowered.

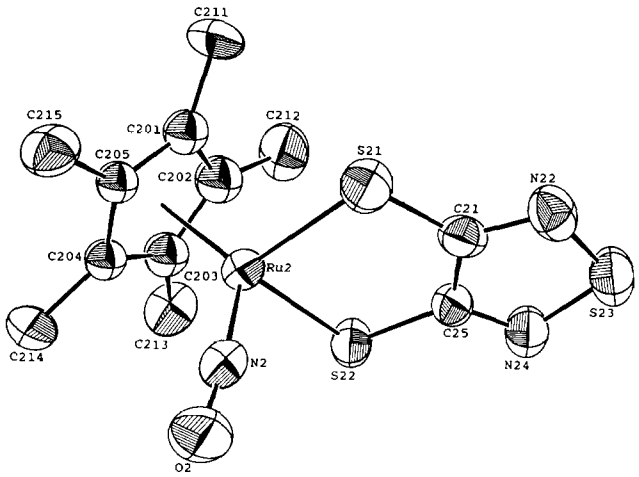


Fig. 1. ORTEP diagram of one of the molecules of Cp*Ru(NO)(tdas) with the thermal ellipsoids drawn at the 50% probability level.

It is readily seen that the 0/+1 redox couple is quasi-reversible at room temperature with a scan rate of 100 mV $s^{-1}$ based on a calculated current ratio of 0.53. Under these conditions, the $\Delta E_p$ value associated with this wave is 70 mV (see Fig. 2(a)). The reversibility of this redox couple was also examined as a function of both the scan rate and temperature. Increasing $\nu$ to 5 V $s^{-1}$ led to a noticeable improvement in the reversibility of the 0/+1 wave as the current ratio increased to 0.80 (not shown). The effect of temperature on the oxidation is shown in Fig. 2, where $i_{pc}/i_{pa}$ values of 0.81 and 0.91 were calculated from the cyclic voltammograms shown in Fig. 2(b) and (c), which were recorded at 0 and −20 °C, respectively. The electrochemical pathways available to **2** are summarized below in Eq. (2).

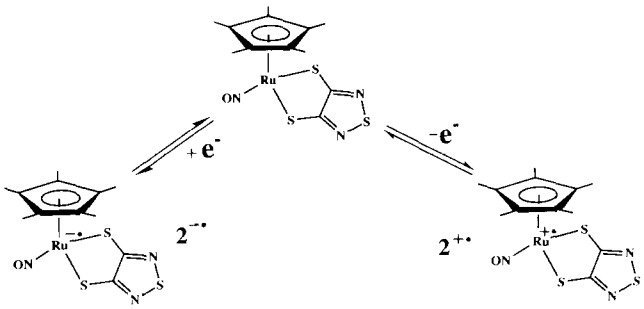


(2)

The scan rate and temperature dependence exhibited by the oxidation wave is consistent with an EC sequence [17,18]. At slow scan rates, the initially generated radical-cation $\mathbf{2}^{\cdot+}$ is consumed by a fast follow-up chemical reaction. The cyclic voltammogram will appear to be reversible when the time scale of the experiment is shortened (fast $\nu$) or when the temperature is reduced. Both of these conditions minimize the rate at which $\mathbf{2}^{\cdot+}$ participates in the deleterious chemical step. At this time the reason(s) for the instability of

Table 3
Selected bond lengths (Å) and angles (°) in Cp*Ru(NO)(tdas) (**2**) [a]

| | | | |
|---|---|---|---|
| *Bond distances* | | | |
| Molecule A | | | |
| Ru(1)–S(11) | 2.371(2) | Ru(1)–S(12) | 2.363(2) |
| Ru(1)–N(1) | 1.758(5) | S(11)–C(11) | 1.723(8) |
| S(12)–C(15) | 1.742(7) | S(13)–N(12) | 1.636(7) |
| S(13)–N(14) | 1.644(7) | O(1)–N(1) | 1.153(8) |
| N(12)–C(11) | 1.329(9) | N(14)–C(15) | 1.30(1) |
| C(11)–C(15) | 1.432(9) | Ru(1)–C(101) | 2.252(6) |
| Ru(1)–C(102) | 2.309(6) | Ru(1)–C(103) | 2.269(6) |
| Ru(1)–C(104) | 2.214(7) | Ru(1)–C(105) | 2.236(7) |
| Molecule B | | | |
| Ru(2)–S(21) | 2.365(2) | Ru(2)–S(22) | 2.374(2) |
| Ru(2)–N(2) | 1.751(6) | S(21)–C(21) | 1.727(8) |
| S(22)–C(25) | 1.746(7) | S(23)–N(22) | 1.650(7) |
| S(23)–N(24) | 1.659(7) | O(2)–N(2) | 1.155(9) |
| N(22)–C(21) | 1.31(1) | N(24)–C(25) | 1.30(1) |
| C(21)–C(25) | 1.432(8) | Ru(2)–C(201) | 2.311(6) |
| Ru(2)–C(202) | 2.249(8) | Ru(2)–C(203) | 2.239(7) |
| Ru(2)–C(204) | 2.245(7) | Ru(2)–C(205) | 2.267(7) |
| *Bond angles* | | | |
| Molecule A | | | |
| S(11)–Ru(1)–S(12) | 87.74(6) | S(11)–Ru(1)–N(1) | 99.9(2) |
| S(12)–Ru(1)–N(1) | 100.2(2) | S(11)–Ru(1)–C(101) | 149.5(1) |
| S(11)–Ru(1)–C(102) | 121.2(1) | S(11)–Ru(1)–C(103) | 89.8(2) |
| S(11)–Ru(1)–C(104) | 90.3(2) | S(11)–Ru(1)–C(105) | 124.2(2) |
| S(12)–Ru(1)–C(101) | 106.5(2) | S(12)–Ru(1)–C(102) | 87.8(2) |
| S(12)–Ru(1)–C(103) | 105.7(2) | S(12)–Ru(1)–C(104) | 142.3(2) |
| S(12)–Ru(1)–C(105) | 143.2(2) | S(22)–Ru(2)–C(201) | 126.1(2) |
| N(1)–Ru(1)–C(101) | 103.7(2) | N(1)–Ru(1)–C(102) | 138.5(2) |
| N(1)–Ru(1)–C(103) | 152.6(3) | N(1)–Ru(1)–C(104) | 117.2(3) |
| N(1)–Ru(1)–C(105) | 92.1(3) | Ru(1)–S(11)–C(11) | 103.4(2) |
| Ru(1)–S(12)–C(15) | 104.0(3) | S(13)–N(14)–C(15) | 106.4(5) |
| S(13)–N(12)–C(11) | 106.7(5) | S(11)–C(11)–N(12) | 123.6(5) |
| Ru(1)–N(1)–O(1) | 169.2(6) | N(12)–C(11)–C(15) | 113.0(6) |
| Molecule B | | | |
| S(21)–Ru(2)–S(22) | 88.03(7) | S(21)–Ru(2)–N(2) | 101.3(2) |
| S(22)–Ru(2)–N(2) | 94.1(2) | S(11)–C(11)–C(15) | 123.4(5) |
| S(21)–Ru(2)–C(201) | 85.6(2) | S(21)–Ru(2)–C(202) | 99.2(2) |
| S(21)–Ru(2)–C(203) | 137.2(2) | S(21)–Ru(2)–C(204) | 143.8(1) |
| S(21)–Ru(2)–C(205) | 107.2(1) | S(22)–Ru(2)–C(202) | 92.6(2) |
| S(22)–Ru(2)–C(203) | 90.9(2) | S(22)–Ru(2)–C(204) | 121.7(2) |
| S(22)–Ru(2)–C(205) | 151.2(2) | N(2)–Ru(2)–C(201) | 139.6(3) |
| N(2)–Ru(2)–C(202) | 158.6(3) | N(2)–Ru(2)–C(203) | 121.4(3) |
| N(2)–Ru(2)–C(204) | 97.0(3) | N(2)–Ru(2)–C(205) | 106.3(3) |
| Ru(2)–S(21)–C(21) | 103.8(2) | Ru(2)–S(22)–C(25) | 103.2(2) |
| Ru(2)–N(2)–O(2) | 171.0(6) | S(23)–N(24)–C(25) | 107.2(4) |
| S(23)–N(22)–C(21) | 107.9(4) | S(21)–C(21)–N(22) | 124.9(5) |
| S(21)–C(21)–C(25) | 122.6(5) | N(24)–C(25)–C(21) | 114.5(6) |

[a] Numbers in parentheses are e.s.d.s in the least significant digits.

$[Cp^*Ru(NO)(tdas)]^{\cdot+}$ is not known, and the synthesis and reactivity study of additional complexes derived from the 'Cp*Ru(NO)' fragment are planned in order to assist us in the examination of the oxidation process.

The electrochemical response of **2** at a rotated disk electrode was next examined in order to ascertain the electron stoichiometry of each redox wave. The RDE voltammogram, which was obtained in MeCN solvent containing 0.25 M TBAP at room temperature, is shown in Fig. 3. The presence of well-defined half-wave potentials ($E_{1/2}$) at 0.97 and −1.06 V are in full agreement with the redox processes assigned by cyclic voltammetry. The electron stoichiometry associated with the oxidation and reduction waves was determined by constructing plots of $E$ versus log $[(i_d - i)/i]$. For the 0/+1 redox wave, a slope of 55.5 mV was computed, which is close to the theoretically predicted value of 59.1 mV for a one-electron oxidation [19,20]. The reduction wave exhibited a slope of 74.5 mV, a value slightly larger than that expected for a Nernstian process. However, the one-electron nature of the 0/−1 redox couple is firmly established given the similarity in the absolute value for the limiting current (i.e. $|i_d|$) found for both redox waves.

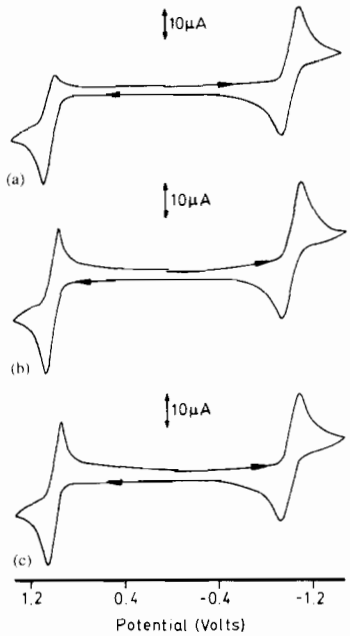


Fig. 2. Cathodic scan cyclic voltammogram of $\sim 1\times10^{-3}$ M Cp*Ru(NO)(tdas) in MeCN containing 0.25 M TBAP at 100 mV $s^{-1}$ at (a) room temperature, (b) 0 °C and (c) −20 °C.

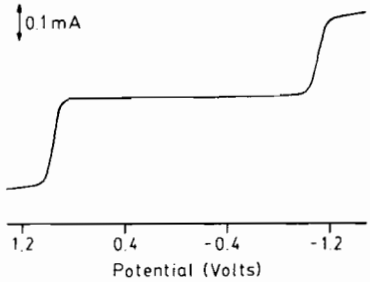


Fig. 3. Rotating disk electrode voltammogram of $\sim 2.5\times10^{-3}$ M Cp*Ru(NO)(tdas) in MeCN at room temperature containing 0.25 M TBAP at 100 mV $s^{-1}$ and $\omega = 1000$ rpm.

Fig. 4 shows the cyclic voltammograms of Cp*Ru(NO)(tdas) in THF and provides evidence for the possible bending of the nitrosyl ligand upon one electron reduction. The data are collected in Table 4. In Fig. 4 the CVs of Cp*Ru(NO)(tdas) reveal that the

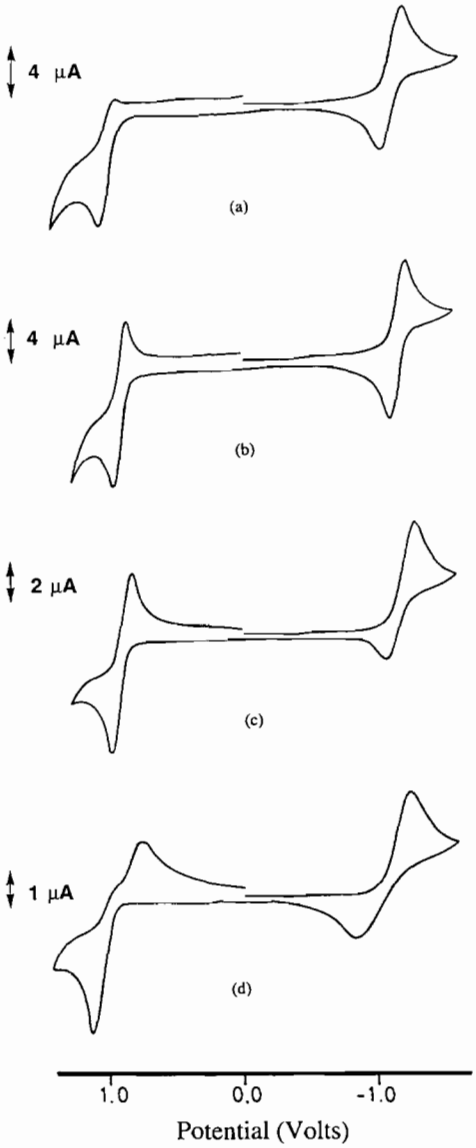


Fig. 4. Cathodic scan cyclic voltammogram of $\sim 1\times10^{-3}$ M Cp*Ru(NO)(tdas) in THF containing 0.25 M TBAP at 100 mV $s^{-1}$ at (a) room temperature, (b) 0 °C, (c) −20 °C and (d) −67 °C.

0/+1 redox gradually becomes more reversible as the temperature is changed from room temperature to −20 °C, changing from an initial ratio of 0.46 to 0.89. Further cooling to −67 °C produces a totally irreversible redox couple. The possibility of high resistance derived from the solvent being responsible for the observed chemistry may be eliminated as internally added ferrocene exhibits a $\Delta E_p$ value of ~85 mV at −67 °C. As with the oxidation couple in MeCN solvent, the nature of the decomposition reaction remains unclear.

The effect of temperature on the 0/−1 redox couple in **2** at room temperature and 0 °C is very similar, and this redox couple may be regarded as reversible given the measured current ratio associated this couple at each temperature. Temperatures below 0 °C dramatically affect the 0/−1 redox couple as seen in Fig. 4(c) and (d), which have been recorded at −20 and −67 °C, respectively. The CV behavior in Fig. 4(c) and (d) is consistent with a structural change that may involve the bending of the nitrosyl ligand. Here the rate constant ($k_{-1}$) for the bent-to-linear nitrosyl transformation is slow and observable at low temperatures in THF solvent. A scenario that accounts for this irreversible CV behavior and is outlined in Eq. (3). Such a scheme has been shown to be operative in the reduction chemistry reported for $CpM(CO)_2(NO)$ (where M = Cr, Mo) [21] and Cp*Ru(NO)(mnt) [14].

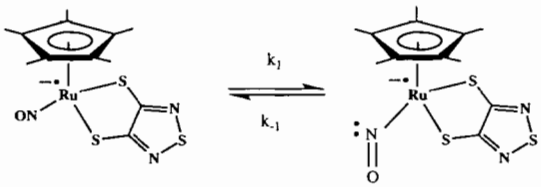


(3)

## 2.4. Extended Hückel molecular orbital calculations

The orbital composition of the HOMO and LUMO in Cp*Ru(NO)(tdas) was determined by extended Hückel molecular orbital calculations. Fig. 5 shows the three-dimensional CACAO [22] drawing of the HOMO and LUMO in Cp*Ru(NO)(tdas). The HOMO, which is found at ~ −11.3 eV, is primarily a ruthenium-based orbital, with the major metal contribution being derived from the $d_{x^2-y^2}$ orbital. Hybridization of the HOMO with ruthenium py and $d_{z^2}$ character serves to further shape this orbital. The extended Hückel data also reveal minor contributions to the HOMO from the thiolate atoms, the carbons of the tdas ligand, and the Cp* ring carbons. The former two of these interactions are repulsive in nature, much like those observed in the cyclopentadienyl complex $CpMo(NO)(SH)_2$ reported by Ashby and Enemark, and Hunter et al. [23]. A similar HOMO orbital composition has been found by us in the related cyclopentadienyl complex Cp*Ru(NO)(mnt) [14]. The observed 0/+1 redox couple in **2** is consistent with an oxidation that occurs at a ruthenium-based orbital as reported for a variety of $d^6$ ruthenium complexes [24].

The LUMO in Cp*Ru(NO)(tdas) occurs at ~ −9.6 eV and reveals the presence of major contributions from the nitrogen atom of the nitrosyl ligand, the ruthenium atom and the tdas ligand. The LUMO is best described as a ligand-based orbital, where the $d_{zy}$ orbital of the ruthenium exhibits $d\pi$–$p\pi$ out-of-phase overlap with both the nitrosyl and tdas ligands. When just the tdas ligand in the LUMO is considered, it is readily seen that four nodes are present. This same nodal pattern is observed in the LUMO of the parent dithiol complex 3,4-bis(thiol)-1,2,5-thiadiazole when considered by Hückel theory [25]. We note that an

Table 4
Cyclic voltammetric data for Cp*Ru(NO)(tdas) [a]

| Solvent/Temp. [b] | Redox couple [c] | | | | | | | |
|---|---|---|---|---|---|---|---|---|
| | 0/+1 | | | | 0/−1 | | | |
| | $E_{pa}$ | $E_{pc}$ | $i_{pc}/i_{pa}$ | $E_{1/2}$ | $E_{pc}$ | $E_{pa}$ | $i_{pa}/i_{pc}$ | $E_{1/2}$ |
| MeCN/r.t. | 1.02 | 0.95 | 0.53 | 0.99 | −1.10 | −1.01 | 1.0 | −1.06 |
| MeCN/0 °C | 1.02 | 0.96 | 0.81 | 0.99 | −1.10 | −0.97 | 1.0 | −1.04 |
| MeCN/−20 °C | 1.02 | 0.95 | 0.91 | 0.99 | −1.10 | −0.98 | 1.0 | −1.04 |
| THF/r.t. | 1.09 | 1.01 | 0.46 | 1.05 | −1.11 | −1.00 | 1.0 | −1.06 |
| THF/0 °C | 0.99 | 0.92 | 0.80 | 0.96 | −1.18 | −1.08 | 0.90 | −1.13 |
| THF/−20 °C | 0.99 | 0.89 | 0.89 | 0.94 | −1.22 | −1.04 | [d] | [d] |
| THF/−67 °C | 1.13 | 0.84 | [d] | [d] | −1.17 | −0.80 | [d] | [d] |

[a] All cyclic voltammograms were recorded in solutions containing 0.25 M TBAP at a scan rate of 0.1 V $s^{-1}$. Potentials are in volts relative to a silver wire quasi-reference electrode, calibrated against added ferrocene.

[b] All temperatures were measured with the aid of a digital thermometer and are considered to be accurate within ±1 °C.

[c] $E_{pa}$ and $E_{pc}$ refer to the anodic and cathodic peak potentials for a given redox couple. The half-wave potential $E_{1/2}$, which represents the chemically reversible redox couple, is defined as $(E_{pa}+E_{pc})/2$.

[d] No reverse redox couple was observed.

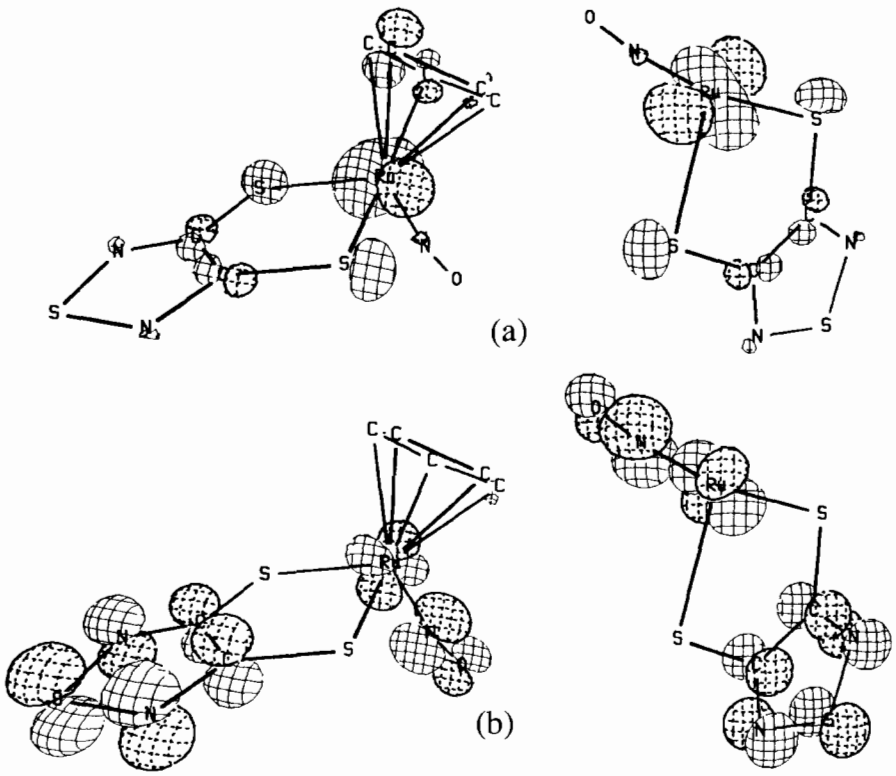


Fig. 5. CACAO drawings of the HOMO (a) and LUMO (b) of Cp*Ru(NO)(tdas). The Cp*-methyl groups have been eliminated from the side-view drawings on the left while the Cp* ring has been eliminated from the top-view drawing on the right.

earlier polarographic study has shown that the parent heterocycle 1,2,5-dithiadiazole and various 3,4-substituted derivatives exhibit one-electron reductions over the potential range of 1.44 to 2.60 V versus $Ag/Ag^+$ [26]. While these data suggest that the tdas ligand in **2** could serve as the site of the initial electron accession from the electrode, the solvent- and temperature-dependent cyclic voltammetry data support a pathway involving nitrosyl bending. Future ESR studies are planned in order to fully address the spin density on the tdas and RuNO moieties in $\mathbf{2}^{\cdot-}$.

## 3. Conclusions

The synthesis, solid-state structure and electrochemical properties of Cp*Ru(NO)(tdas) have been pre-

sented. Cp*Ru((NO)(tdas) exhibits diverse quasi-reversible oxidation and reduction chemistry, as determined by cyclic voltammetric studies. The behavior of the one-electron reduction is controlled by both the nature of the reaction solvent and the temperature, with evidence being presented for the possible bending of the nitrosyl ligand in $2^{\cdot-}$. Molecular orbital calculations have been carried out and the composition of the HOMO and LUMO levels has been established.

## 4. Experimental

Disodium 1,2,5-thiadiazole-3,4-dithiol ($Na_2$tdas) [10] and Cp*Ru(NO)$Cl_2$ [9] were synthesized by following the reported procedures. Methanol was degassed by argon prior to each reaction. THF and benzene were distilled from sodium/benzophenone while $CH_2Cl_2$ and MeCN were distilled from $CaH_2$. All solvents were distilled under argon using inert-atmosphere techniques and stored in Schlenk vessels equipped with Teflon stopcocks [27]. The tetra-n-butylammonium perchlorate, which was purchased from Johnson Matthey Electronics, was recrystallized from an ethyl acetate/petroleum ether mixture, followed by drying under vacuum for 72 h. The C and H combustion analysis was performed by Atlantic Microlab, Atlanta, GA.

The $^1$H and $^{13}$C NMR spectra were recorded on a Varian 200 VXR spectrometer at 200 and 50 MHz, respectively. IR spectra were recorded on a Nicolet 20 SXB FT-IR spectrometer using 0.1 mm NaCl cells.

### 4.1. Synthesis of Cp*Ru(NO)(tdas)

To 25 ml of degassed MeOH containing 0.20 g (0.60 mmol) of Cp*Ru(NO)$Cl_2$ was added 0.14 g (~0.71 mmol) of $Na_2$tdas. The reaction mixture was stirred overnight at room temperature, after which the solvent was removed and the solid was extracted with $CH_2Cl_2$. The desired product was subsequently isolated by chromatography over silica gel using $CH_2Cl_2$ as the eluant. The analytical sample and crystals suitable for single-crystal X-ray diffraction analysis were obtained from a $CH_2Cl_2$ solution of **2** that had been layered with pentane. Yield 0.15 g (61%). IR ($CH_2Cl_2$): 1769 (s, NO) cm$^{-1}$. $^1$H NMR ($CDCl_3$): $\delta$ 1.86 (Cp*). $^{13}$C NMR ($CDCl_3$): $\delta$ 9.5 (Me), 109.5 (Cp* ring), 169.6 (tdas ring). *Anal.* Found C, 34.75; H, 3.61. Calc. for $C_{12}H_{15}N_3ORuS_3$: C, 34.78; H, 3.62%.

### 4.2. X-ray crystallography

A black crystal of Cp*Ru(NO)(tdas) of dimensions 0.05 mm×0.12 mm×0.32 mm was sealed inside a Lindemann capillary tube and mounted on the goniometer of an Enraf-Nonius CAD-4 diffractometer. The radiation employed was Mo K$\alpha$ monochromatized by a single crystal of graphite. Cell constants were obtained from a least-squares refinement of 25 reflections with $2\theta > 32°$. Intensity data in the range $2.0 \leqslant 2\theta \leqslant 44.0°$ were collected at room temperature using the $\omega$-scan technique in the variable-speed mode and were corrected for Lorentz, polarization and absorption (DIFABS). Three reflections (1500, 040, 008) were measured after every 3600 s of exposure as a check of crystal integrity. The structure was solved by using standard Patterson techniques, which revealed the position of the ruthenium atom. All remaining non-hydrogen atoms were located with difference Fourier maps and full-matrix least-squares refinement. With the exception of the cyclopentadienyl carbons, all non-hydrogen atoms were refined anisotropically. Refinement converged at $R = 0.0338$ and $R_w = 0.0373$ for 3151 unique reflections with $I > 3\sigma(I)$.

### 4.3. Cyclic and rotating disk electrode voltammetry

A PAR model 273 potentiostat/galvanostat was used to collect all the reported cyclic and rotating disk electrode voltammograms. All cyclic voltammograms were recorded in the positive feedback mode to reduce unwanted solution resistance. The CV cell used was of airtight design and based on a three-electrode configuration, allowing all cyclic voltammograms to be recorded free from oxygen and moisture. The CV studies were conducted with platinum disk (area = 0.0079 cm$^2$) working and auxiliary electrodes. The RDE voltammogram was recorded in a Vacuum Atmospheres Dribox using a PAR model 616 RDE unit. A platinum disk working electrode (area = 0.126 cm$^2$) was used in the RDE studies. Both the CV and the RDE experiments employed a silver quasi-reference electrode, with all potential data being referenced to the formal potential of the ferrocene/ferrocenium (internally added) redox couple run under identical conditions, taken to have an $E_{1/2} = 0.307$ V [17].

### 4.4. Extended Hückel molecular orbital calculations

The HOMO and LUMO levels in Cp*Ru(NO)(tdas) were calculated by using the original extended Hückel program written by Hoffmann [28] as modified by Mealli and Proserpio [22]. The atomic parameters used in this study were taken from the CACAO drawing program with all bond distance and angles being taken from the X-ray crystallographic coordinates.

## 5. Supplementary material

Listing of observed and calculated structure factor amplitudes, tables of anisotropic thermal parameters,

and idealized hydrogen parameters, and X-ray information are available from the authors upon request.

## Acknowledgements

We are especially grateful to Professor Carlo Mealli for providing us with a copy of his CACAO graphics program, and we thank the Robert A. Welch Foundation (B-1202-SGB and B-1039-MGR) and the UNT Faculty Research Program for continued financial support.

## References

[1] R.P. Burns and C.A. McAuliffe, *Adv. Inorg. Chem. Radiochem.*, *22* (1979) 303.
[2] R. Eisenberg, *Prog. Inorg. Chem.*, *12* (1970) 295.
[3] G.N. Schrauzer, *Acc. Chem. Res.*, *2* (1969) 72.
[4] P. Cassoux, L. Valade, H. Kobayashi, A. Kobayashi, R.A. Clark and A.E. Underhill, *Coord. Chem. Rev.*, *110* (1991) 115, and refs. therein.
[5] A. Mueller, *Polyhedron*, *5* (1986) 323.
[6] J.A. Zuleta, M.S. Burberry and R. Eisenberg, *Coord. Chem. Rev.*, *97* (1990) 47.
[7] I. Hawkins and A.E. Underhill, *J. Chem. Soc., Chem. Commun.*, (1990) 1593.
[8] O.A. Dyachenko, S.V. Konovalikhin, A.I. Kotov, G.V. Shilov, E.B. Yagubskii, C. Faulmann and P. Cassoux, *J. Chem. Soc., Chem. Commun.*, (1993) 508.
[9] J.L. Hubbard, A. Morneau, R.M. Burns and C.R. Zoch, *J. Am. Chem. Soc.*, *113* (1991) 9176.
[10] G. Wolmershäuser and R. Johann, *Angew. Chem., Int. Ed. Engl.*, *28* (1989) 920.
[11] J.L. Morris and C.W. Rees, *J. Chem. Soc., Perkin Trans. 1* (1987) 217.
[12] (a) R. Eisenberg and C.D. Meyer, *Acc. Chem. Res.*, *8* (1975) 26; (b) D.M.P. Mingos and D.J. Sherman, *Adv. Inorg. Chem.*, *34* (1989) 292.
[13] (a) V. Gama, R.T. Henriques, G. Bonfait, L.C. Pereira, J.C. Waerenborgh, I.C. Santos, M.T. Duarte, J.M.P. Cabral and M. Almeida, *Inorg. Chem.*, *31* (1992) 2598; (b) V. Gama, R.T. Henriques, M. Almeida, L. Veiros, M.J. Calhorda, A. Meetsma and J.L. de Boer, *Inorg. Chem.*, *32* (1993) 3705.
[14] K. Yang, S.G. Bott and M.G. Richmond, *J. Organomet. Chem.*, (1994) in press.
[15] (a) C.-H. Cheng and R. Eisenberg, *Inorg. Chem.*, *18* (1979) 1418; (b) *18* (1979) 2438; (c) E.G. Megehee, C.E. Johnson and R. Eisenberg, *Inorg. Chem.*, *28* (1989) 2423.
[16] (a) C.G. Pierpont, A. Pucci and R. Eisenberg, *J. Am. Chem. Soc.*, *93* (1971) 3050; (b) R. Eisenberg and C.D. Meyer, *Acc. Chem. Res.*, *8* (1975) 26.
[17] A.J. Bard and L.F. Faulkner, *Electrochemical Methods*, Wiley, New York, 1980.
[18] P.H. Rieger, *Electrochemistry*, Chapman and Hall, New York, 1994.
[19] J. Tomeš, *Collect. Czech. Chem. Commun.*, *9* (1937) 150.
[20] V.G. Levich, *Physicochemical Hydrodynamics*, Prentice Hall: Englewood Cliffs, NJ, 1962.
[21] W.E. Geiger, P.H. Rieger, B. Tulyathan and M.D. Rausch, *J. Am. Chem. Soc.*, *106* (1984) 7000.
[22] C. Mealli and D.M. Proserpio, *J. Chem. Educ.*, *67* (1990) 399.
[23] (a) M.T. Ashby and J.H. Enemark, *J. Am. Chem. Soc.*, *108* (1986) 730; (b) A.D. Hunter, P. Legzdins, F.W.B. Einstein, A.C. Willis, B.E. Bursten and M.G. Gatter, *J. Am. Chem. Soc.*, *108* (1986) 3843.
[24] A.B.P. Lever, *Inorg. Chem.*, *30* (1991) 1980, and refs. therein.
[25] T.A. Albright, J.K. Burdett and M.H. Whangbo, *Orbital Interactions in Chemistry*, Wiley-Interscience, New York, 1985.
[26] E.O. Sherman, Jr., S.M. Lambert and K. Pilgram, *J. Heterocycl. Chem.*, *11* (1974) 763.
[27] D.F. Shriver, *The Manipulation of Air-Sensitive Compounds*, McGraw-Hill, New York, 1969.
[28] (a) R. Hoffmann and W.N. Lipscomb, *J. Phys. Chem.*, *36* (1962) 2179, 3489; (b) R. Hoffmann, *J. Phys. Chem.*, *39* (1963) 1397.